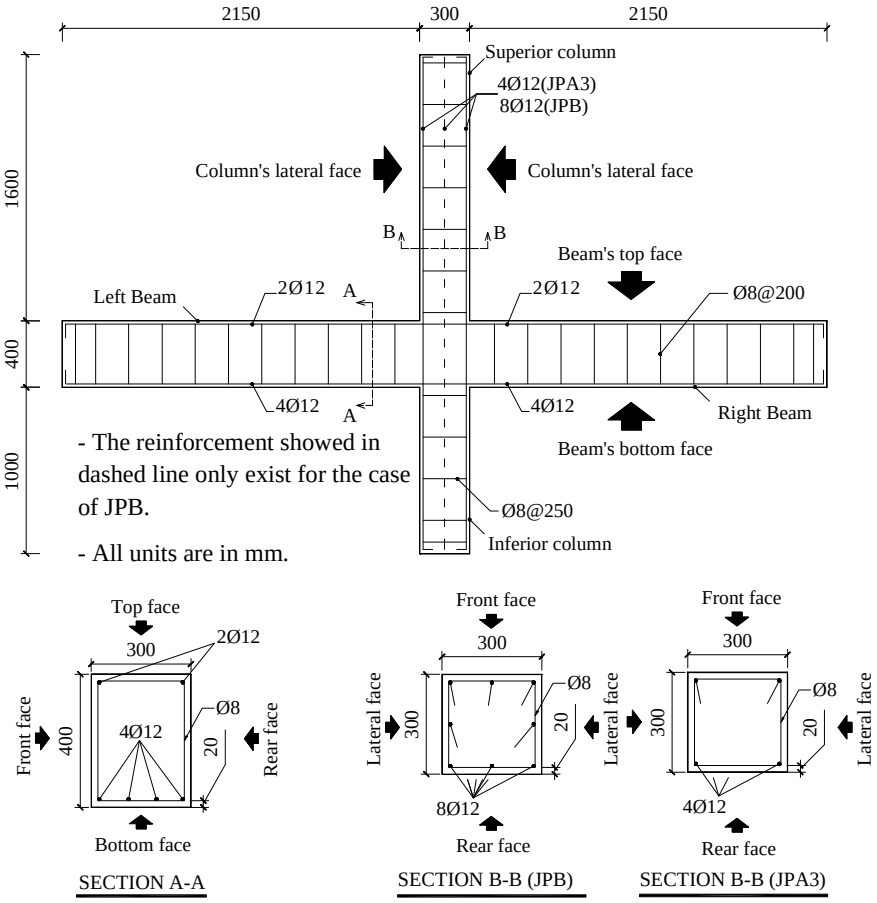

Figure 1: Details of adopted configurations for the interior RC beam-column connections.

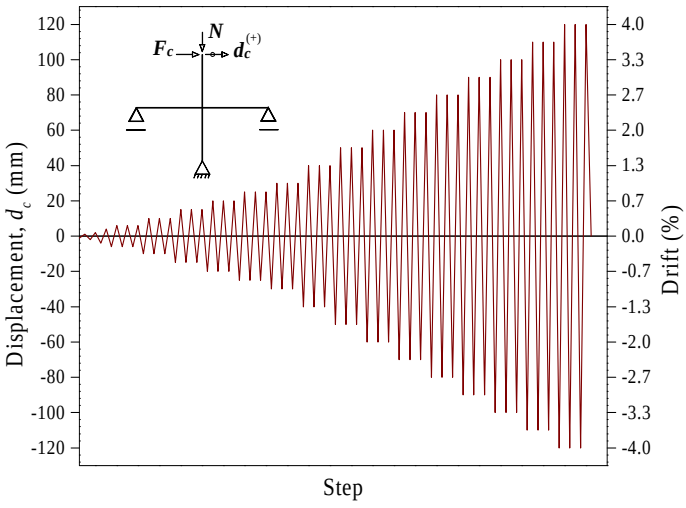

Cycle Numbers	d_c^p (mm)	Max drift (%)
1	±1	0.033
2	±2	0.067
3	±4	0.133
4 to 6	±6	0.20
7 to 9	±10	0.33
10 to 12	±15	0.50
13 to 15	±20	0.67
16 to 18	±25	0.83
19 to 21	±30	1.00
22 to 24	±40	1.33
25 to 27	±50	1.67
28 to 30	±60	2.00
31 to 33	±70	2.33
34 to 36	±80	2.67
37 to 39	±90	3.00
40 to 42	±100	3.33
43 to 45	±110	3.67
46 to 48	±120	4.00

Figure 2: Loading history adopted for the lateral displacement cycles (d_c^p: peak displacement for the corresponding cycle or set of cycles).

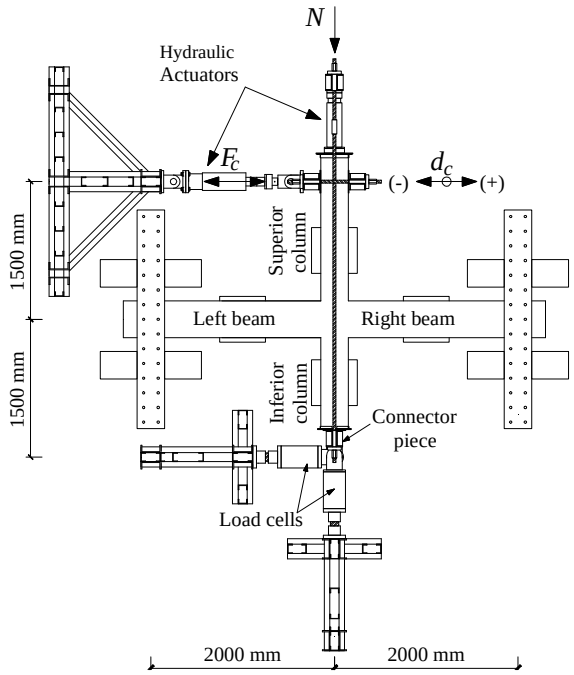

Figure 3: Test setup adopted for the horizontally placed specimens [20]

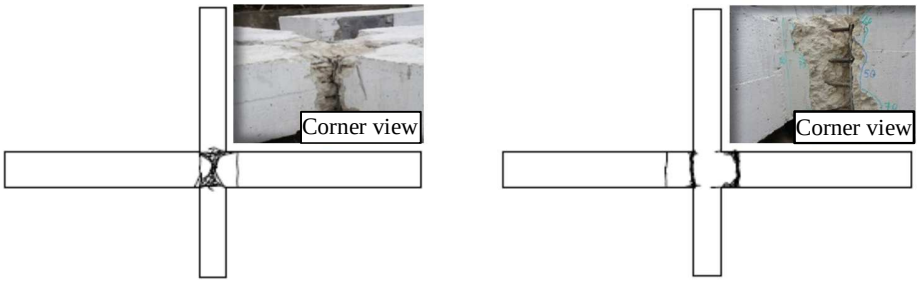

(a) (b)

Figure 4: The extent of damages before retrofitting a) JPA3 and b) JPB.

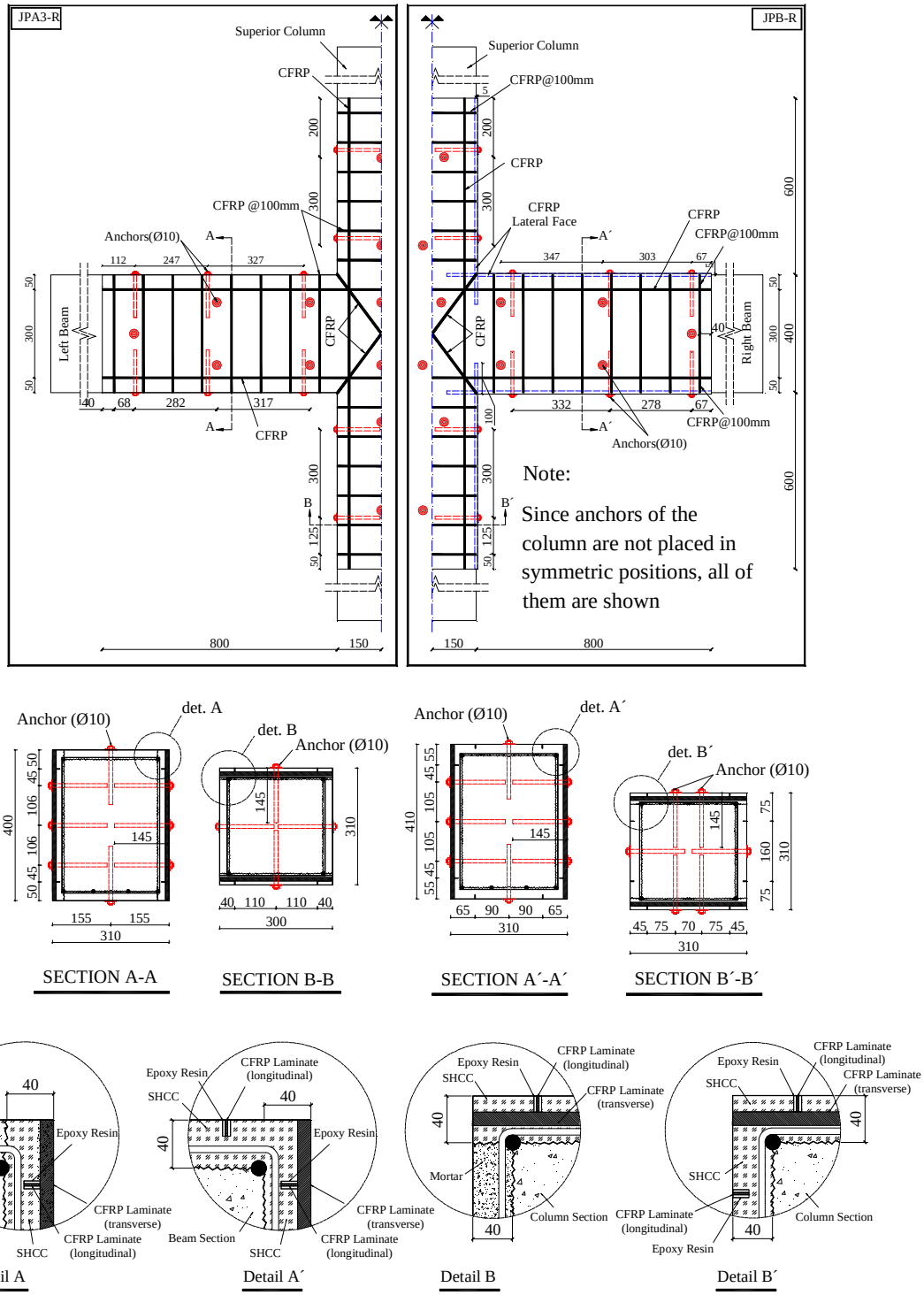

Figure 5: Details of the schemes used for the retrofitting of the damaged specimens (dimensions in mm)

(a) (b)

Figure 6: View of the retrofitted specimens a) JPA3-R and b) JPB-R.

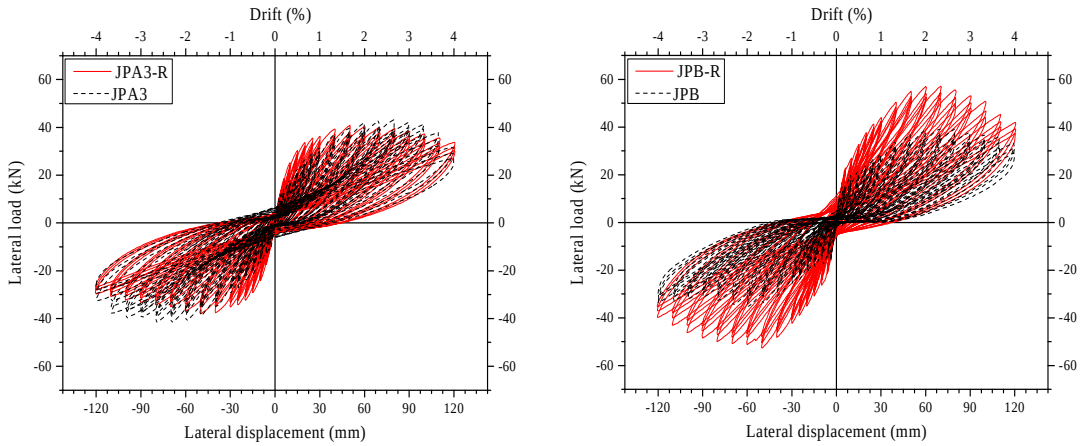

Figure 7: Hysteretic responses of the specimens in the strengthened and virgin states

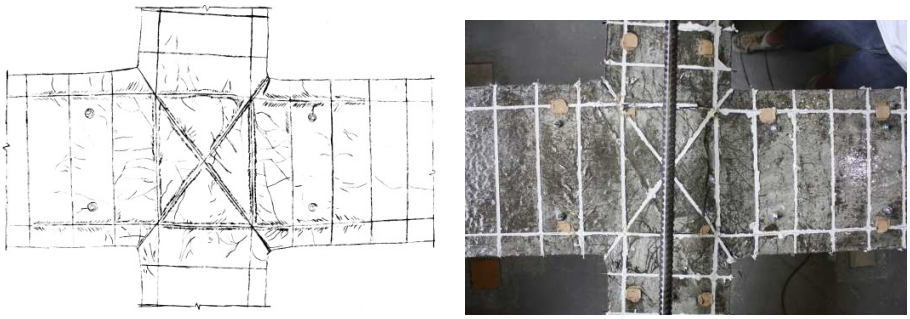

(a) JPA3-R

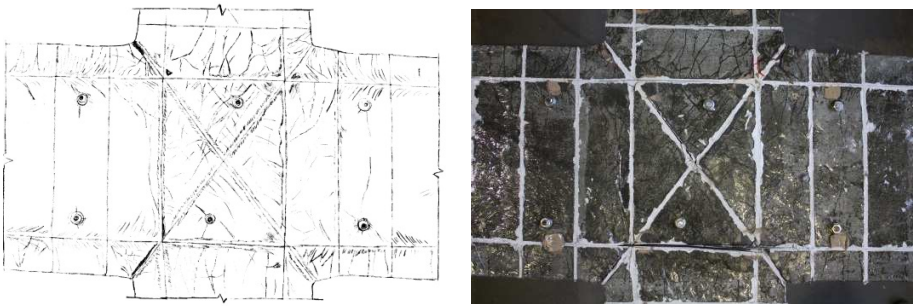

(b) JPB-R

Figure 8: Damage propagation and concentration at the failure of (a) JPA3-R and (b) JPB-R

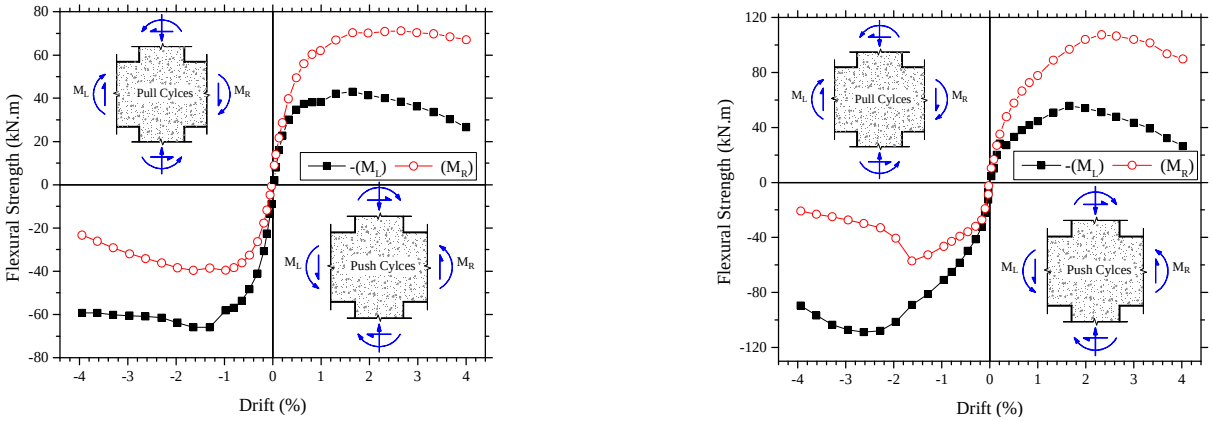

(a) (b)

Figure 9: Development of the resisting bending moment at the interfaces of the beams with columns a) JPA3-R and b) JPB-R

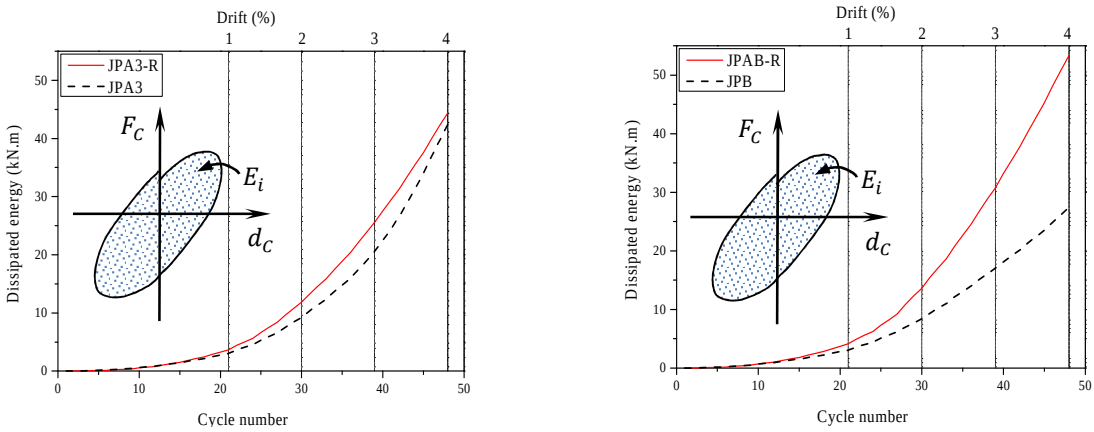

(a) (b)

Figure 10: Evolution of the dissipated energy during the cyclic loading a) JPA3-R and JPA3, and b) JPB-R and JPB.

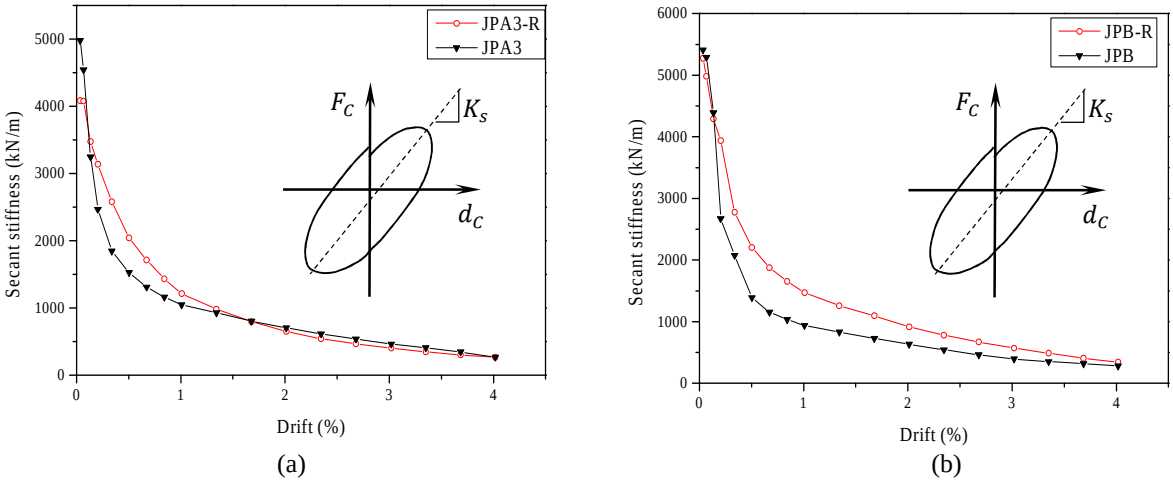

Figure 11: Secant stiffness evolution in a) JPA3-R and JPA3, and b) JPB-R and JPB.

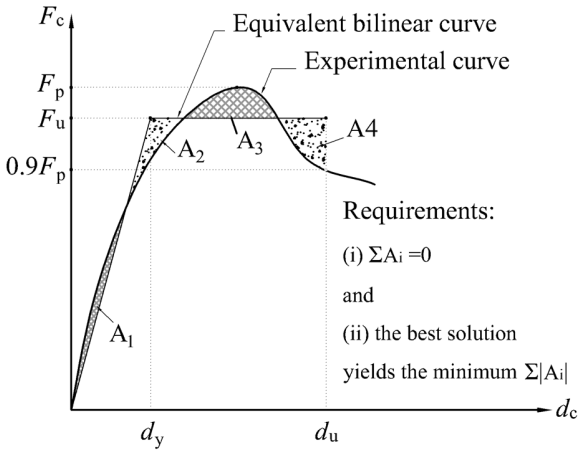

Figure 12: Schematic representation of the definition of the equivalent bilinear curve for the evaluation of the displacement ductility index.

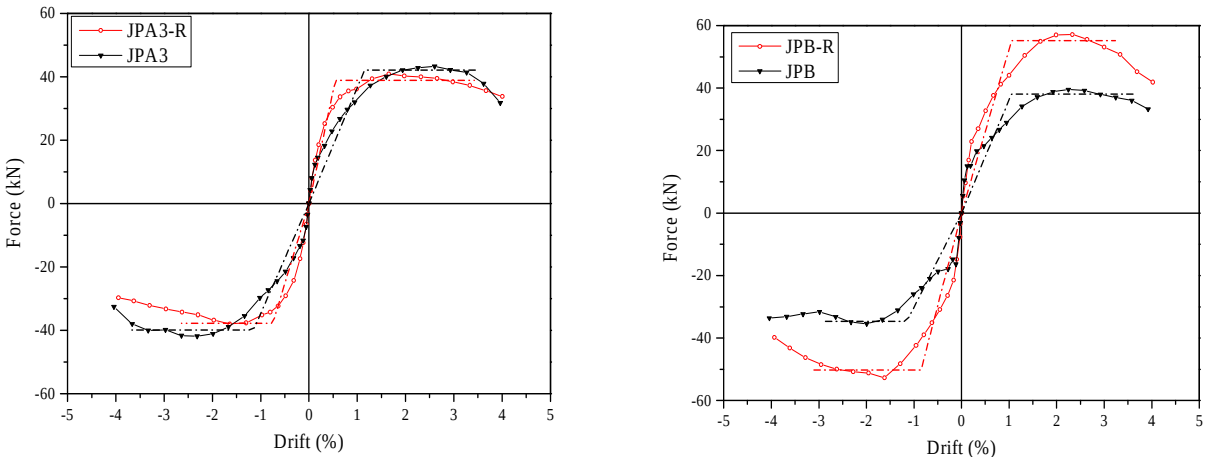

(a) (b)

Figure 13: Envelope of the load versus drift for both the repaired and virgin specimens along with the equivalent elastic-perfectly plastic curves a) JPA3-R and JPA3, and b) JPB-R and JPB.